

Semiclassical dynamical localization and the multiplicative semiclassical propagator

L. Kaplan *

Department of Physics and Society of Fellows,
Harvard University, Cambridge, Massachusetts 02138

We describe an iterative approach to computing long-time semiclassical dynamics in the presence of chaos, which eliminates the need for summing over an exponentially large number of classical paths, and has good convergence properties even beyond the Heisenberg time. Long-time semiclassical properties can be compared with those of the full quantum system. The method is used to demonstrate semiclassical dynamical localization in one-dimensional classically diffusive systems, showing that interference between classical paths is a sufficient mechanism for limiting long-time phase space exploration.

Dynamical localization, the suppression of quantum phase space exploration in a system whose classical analogue is diffusive, is a remarkable example of non-ergodic behavior in quantizations of classically ergodic motion. Since its discovery almost two decades ago, the phenomenon has been discussed and observed in various numerical studies [1,2], and also in experimental settings [3]. Formal connections with Anderson localization in disordered systems have been made [4].

As expected from classical-quantum correspondence, diffusive quantum behavior is observed for times beyond the Ehrenfest time in systems with a diffusive classical limit. Localization then sets in (for dimensions $d < 2$) at a time scale whose dependence on the diffusion constant D and Planck's constant \hbar can be understood by analyzing when interference between classically distinct paths begins to be statistically important. It is thus natural to ask whether phase interference between long classical paths alone is sufficient to produce localization, in the absence of "hard quantum" effects like diffraction and tunneling. Addressing this question has historically been made difficult by the exponential proliferation of paths with time in a chaotic system. For $d = 1$, for example, the localization time scales as D/\hbar^2 , so exact semiclassical calculations all the way to the localization time scale are in practice impossible to carry out for small values of \hbar , where the semiclassical approximation itself is likely to be valid.

An attempt along these lines in Ref. [5] proved somewhat inconclusive, although some preliminary evidence of anomalous long-time behavior was found at 21–27 time steps. This in itself was an impressive calculational feat, made possible by a symbolic dynamics and the piecewise-quadratic nature of the potential. In Ref. [6,7], statistical

properties of long periodic orbits were used to give plausibility arguments for semiclassical localization without performing explicit periodic orbit sums. In Ref. [8], the relationship was examined between the exact quantum propagator in a classically diffusive system, and the semiclassical *one-step* propagator. It is important to note, however, that iteration of a one-step semiclassical propagator does not bear much resemblance to long-time semiclassical dynamics, except insofar as both are (at least at short times) related to the quantum dynamics [9].

In this work we adopt a different approach, based on the idea, recently developed more fully in Ref. [9], that even though semiclassical propagation is not strictly multiplicative, long-time semiclassical dynamics can in fact be well approximated by iteration of intermediate-time propagators, with controllable errors and well-defined convergence properties. In Ref. [9] this approach was used to compute semiclassical dynamics past the Heisenberg time T_H (where individual eigenstates and eigenvalues can be resolved), for a system with $T_H = 256$, without exponential expenditure of computational effort. Good convergence properties with decreasing \hbar allowed for direct comparison between quantum and semiclassical stationary properties, such as long-time transport, spectra, and eigenstates. In the present work we do not directly use any of the results of Ref. [9], but the interested reader is directed there for a more complete discussion of the underlying ideas.

We begin by defining $A_t(i, j)$ to be the semiclassical propagator matrix taking quantum state j to quantum state i in time t (computed using the Gutzwiller–van Vleck semiclassical expression). Unlike the corresponding quantum propagator $U_t(i, j)$, A_t is not unitary, nor is it multiplicative, e.g. $A_t \neq (A_{t/2})^2$. We can, however, easily estimate the deviation from exact multiplicativity of the semiclassical propagator, at least in the caustic-free case. We define the natural basis-independent L_2 norm,

$$\|A - B\|^2 = \frac{1}{N} \sum_{i,j=1}^N |A_{ij} - B_{ij}|^2, \quad (1)$$

where the normalization ensures that the norm of a unitary operator is one. We can then write

$$\|A_t - (A_{t/2})^2\|^2 = O(\hbar^\alpha), \quad (2)$$

where for smooth dynamics, we have the exponent $\alpha_{\text{smooth}} = 2$. This can be seen by noting that A_t is exactly given by combining two $A_{t/2}$ propagators, as long as the intermediate integration at time $t/2$

*kaplan@physics.harvard.edu

is performed by stationary phase. The relative error between performing the intermediate integral exactly $[(A_{t/2})^2(x, y) = \int dz A_{t/2}(x, z) A_{t/2}(z, y)]$ and by stationary phase $[A_t(x, y) = \int_{\text{sp}} dz A_{t/2}(x, z) A_{t/2}(z, y)]$ scales as \hbar (this being the order of the subleading term in the stationary phase expansion); thus $\alpha_{\text{smooth}} = 2$ [9].

In the case of a discontinuity in the underlying classical dynamics, which is to be considered in the present work, the situation is rather different. However, the general approach applies also to this case. In expanding around each of the stationary paths that contribute to $A_t(x, y)$, the region around the stationary phase point where the phase is slowly varying scales as $\hbar^{1/2}$. Thus, for a stationary intermediate point y within $O(\hbar^{1/2})$ of a discontinuity in the potential (or in its first derivative), the exact integral gets cut off within the region of gaussian integration, and the relative error between the full integral and the stationary phase approximation is of order unity. It is easy to see that for small \hbar this diffractive effect dominates the effect of the subleading terms in the expansion (which as we saw lead to $\alpha_{\text{smooth}} = 2$), and results in

$$\alpha_{\text{discontinuous}} = 1/2. \quad (3)$$

For long times t , many classical paths must be summed over to obtain the semiclassical propagator; here we are of course assuming that errors in the sum over paths add no more coherently than the actual contributions themselves.

The next step is to extend Eq. 2 to the more general form

$$\|A_t - (A_{t/M})^M\|^2 = O(M\hbar^\alpha) = O\left(\left(\frac{t}{M}\right)^{-1} t\hbar^\alpha\right), \quad (4)$$

which follows from assuming the successive errors in replacing $M - 1$ stationary phase integrals by exact ones to add incoherently. The assumption of incoherent addition of errors breaks down for very large M (specifically, for M greater than \hbar^{-1} , the Heisenberg time measured in units of the shortest periodic orbit [9]). However, the higher-order corrections in M will not be relevant for our purposes.

Eq. 4 allows successive controlled approximations to be computed to the exact semiclassical dynamics by taking $t/M \gg 1$ (this produces values much closer to the semiclassical than to the quantum results). Of course, taking $M \rightarrow \infty$ ($t/M \ll 1$) in the expression $(A_{t/M})^M$, we instead recover the quantum propagator, as in the Feynman path integral formalism. The intermediate case $t/M \sim 1$ (as in the Bogomolny surface of section approach [10]) produces a long-time dynamics which is strictly speaking neither quantum nor semiclassical, and provides an interpolation between the two worlds.

The scaling properties of the iterative semiclassical approximation with \hbar , time t , and ‘‘quantization time’’

$T_Q \equiv t/M$, as expressed in Eq. 4 above, hold even for times t beyond the Heisenberg time of the system. These scaling properties, based on power-counting arguments, have been extensively tested numerically in [9]. One qualification is that while for $\alpha = 2$ and $T_H \sim \hbar^{-1}$ the approximation at the Heisenberg time using fixed T_Q gets better and better as $\hbar \rightarrow 0$, in the present situation we have $\alpha = 1/2$ and $T_H \sim \hbar^{-2}$, so as \hbar gets small we need larger T_Q to preserve the accuracy of the approximation.

We are now ready to apply the above outlined formalism to the case at hand: dynamical localization in one-dimensional systems. We consider a kicked map [1,11] on a cylindrical phase space $0 \leq q < 2\pi$, $-\infty < p < \infty$,

$$\begin{aligned} \tilde{p} &= p - V'(q) \\ \tilde{q} &= q + \tilde{p} \bmod 2\pi, \end{aligned} \quad (5)$$

with kick potential

$$V(q) = -\frac{1}{2}K(q - \pi)^2 + B \cos q \quad (0 \leq q < 2\pi) \quad (6)$$

turned on momentarily once every time step. Locally the dynamics looks everywhere like an inverted harmonic oscillator with a sinusoidal perturbation (as long as $B < K$), except for a discontinuity in the impulse at $q = 0$. The classical motion is completely chaotic, and diffusive in p ,

$$\langle (p - p_0)^2 \rangle_{\text{classical}} = Dt, \quad (7)$$

with diffusion constant

$$D = \langle (V')^2 \rangle = \frac{1}{2} \left[\left(\frac{2\pi^2 K^2}{3} \right) + B^2 - 4KB \right]. \quad (8)$$

The quantization of Eq. 5 is straightforward [1,11]. Choosing periodic boundary conditions in q -space, we have a momentum basis given by $p_n = n\hbar$, $n = -\infty \dots \infty$. The dynamics is given by a unitary one-step propagator

$$U = e^{-i\tilde{p}^2/2\hbar} e^{-iV(\tilde{q})/\hbar}. \quad (9)$$

Because the quantum dynamics (as well as the classical) is symmetric under parity [$p \rightarrow -p$, $q \rightarrow 2\pi - q$], we will in what follows focus only on the even sector $|p\rangle_{\text{even}} = (|p\rangle + |-p\rangle)/\sqrt{2}$, $p > 0$. This eliminates the problem of tunneling between positive and negative momenta.

The semiclassical dynamics (in the absence of caustics and Maslov phases, which are conveniently avoided by taking $B < K$ in Eq. 6) is given by the standard Gutzwiller-van Vleck propagator

$$\begin{aligned} A_{\text{sc}}(p', p, t) &= \left[\frac{1}{2\pi i \hbar} \right]^{d/2} \sum_j \left| \det \frac{\partial^2 S_j(p, p', t)}{\partial p \partial p'} \right|^{1/2} \\ &\times \exp \frac{iS_j(p, p', t)}{\hbar}, \end{aligned} \quad (10)$$

where S_j is the action for classical path j taking p to p' , and the determinant is the corresponding classical probability density. We can now use Eq. 10 to evaluate the semiclassical propagator matrices A_{T_Q} for various “quantization times” T_Q [9], and then iterate to obtain $A_t \approx (A_{T_Q})^{t/T_Q}$. As $T_Q \rightarrow t$, we obtain the exact semiclassical behavior. In general, though, we only need to take T_Q large enough to obtain the desired level of convergence to the true long-time behavior. The behavior of the iterative semiclassical limit as T_Q becomes large can be compared with the quantum dynamics as given by $U_t = U^t$ (Eq. 9).

The numerical results of this localization study are presented in Figs. 1, 2. In Fig. 1, we choose a piecewise linear map, with parameters $K = 1.073$, $B = 0.0$ in the kick potential of Eq. 6. In Fig. 2, a sinusoidal term is added to the potential: $K = 1.073$, $B = 0.52$. In both cases, the quantum and semiclassical calculations are performed with $\hbar = 0.293$ (note that this takes us well into the semiclassical regime: the relevant expansion parameter is $\hbar/(2\pi)^2$, since $(2\pi)^2$ is the area of a unit cell in phase space). We can now compute $\langle (n - n_0)^2 \rangle$, the spread in momentum space in units of \hbar , as a function of time ($n = p/\hbar$).

More explicitly, given a propagator G_t , whether quantum or semiclassical, we define

$$\langle (n - n_0)^2 \rangle = \left\langle \frac{\sum_i |\langle i | G_t | j \rangle|^2 \left(\frac{p_i}{\hbar} - \frac{p_j}{\hbar} \right)^2}{\sum_i |\langle i | G_t | j \rangle|^2} \right\rangle_j \quad (11)$$

The average over j is performed over initial momenta far from 0 and also far from the edge of the numerical lattice.

The classical diffusion result given by Eqs. 7, 8 appears on the log-log plot in Figs. 1, 2 as a straight line of slope one. The full quantum calculation is seen in the dashed curve, which in each case is seen to turn over and approach a constant after the localization time $T_{\text{loc}} = D/\hbar^2$. This theoretically expected value of T_{loc} (which is also equal to the predicted RMS spread in momentum at infinite time in units of \hbar , the square root of the quantity plotted in Figs. 1,2) is given by $T_{\text{loc}} = 44.1$ in Fig. 1 and $T_{\text{loc}} = 32.7$ in Fig. 2. All these predictions are in reasonable agreement with the full quantum numerics.

We now proceed to the semiclassical analysis. The dotted curve in each of the two Figures represents the momentum spreading given by iteration of the one-step semiclassical propagator A_1 . This does not closely follow the full quantum (or, as we shall soon see, the exact semiclassical result), and the behavior of this quantity in Fig. 2 is particularly erratic.

Now, guided by Eq. 4, we look for convergence to the exact semiclassical answer as the quantization time $T_Q = t/M$ is taken to be much greater than one. Specifically, in Fig. 1 we plot as solid lines the calculations with $T_Q = 7, 8, 9$ (i.e. we take successive approximations $A_t \approx (A_7)^{t/7}$, etc.). We see that the agreement between

the three calculations is very good, strongly suggesting that convergence has been achieved. The semiclassical calculation begins to deviate from the quantum sometime around T_{loc} ; nevertheless it does very clearly localize at a well defined momentum spread somewhat larger than that given by the quantum calculation. (Some difference in the details of the end of classical diffusion for the quantum and semiclassical calculations is not surprising. One should note here for example that the discontinuity in the kick potential will have a diffractive effect on the quantum dynamics, one which will not be present in the semiclassical approximation.)

In Fig. 2, the $T_Q \rightarrow \infty$ convergence to the exact long-time semiclassical dynamics is found to be somewhat slower (calculations with $T_Q = 8, 9, 10$ are plotted as solid lines). Nevertheless, up until $t \approx 200 \approx 6T_{\text{loc}}$, the three curves are in very good agreement, with uncertainty small not only compared to their common deviation from classical diffusion (straight line), but also compared to their common distance from the quantum curve (dashed). The evidence for localization is very clear in this case also, as is the failure of the one-step iterative approximation (dotted curve) to reproduce long-time semiclassical behavior.

As an additional test of semiclassical localization at very long times, we consider the eigenstates of the successive propagators A_{T_Q} as $T_Q \rightarrow \infty$. In the absence of interference effects (i.e. considering each A_{T_Q} simply as a band random matrix of band width $\sqrt{DT_Q/\hbar}$), we would expect the momentum spread $(\delta p)^2$ of the typical eigenstate to increase linearly with T_Q . In fact, however, phase interference between classical paths turns out to be very important indeed, and the average RMS width of the eigenstates of A_{T_Q} is found not to increase significantly with T_Q once $T_Q \gg 1$. In Fig. 3, the mean RMS width (in units of \hbar) of A_{T_Q} eigenstates centered well away from the edge of the numerical lattice is plotted vs. the quantization time T_Q . Parameters are the same as in the previous two figures: plusses are used for the $B = 0.0$ case (corresponding to Fig. 1) and squares for $B = 0.52$ (as in Fig. 2). The result using the $T_Q = 1$ one-step iterated semiclassical propagator is also plotted, as is the quantum momentum spread at $T_Q = 0$. We see localization at large T_Q for both sets of parameters; in each case, the localization length is somewhat larger semiclassically as compared to the quantum calculation. The result obtained using $T_Q = 1$ is intermediate between semiclassical and quantum in both cases.

We can test the scaling of the semiclassical localization length with the diffusion constant by comparing the results for $B = 0.0$ and $B = 0.52$. The ratio of semiclassical localization lengths for these two parameters is found to be 1.32 (using $T_Q = 6$); analytically we predict 1.35.

The behavior of the semiclassical localization with \hbar has also been investigated, and we find that the localization length increases roughly in accordance with the

theoretical predictions of dynamical localization theory. However, the semiclassical localization length does grow somewhat more slowly with $1/\hbar$ than the quantum localization length, apparently leading to a convergence between these quantities at small \hbar . Thus, for $B = 0.52$ and using $T_Q = 6$ we find a ratio of 1.66 between the long-time semiclassical and quantum localization lengths; reducing \hbar by a factor of 2 causes this ratio to drop to 1.35. Unfortunately we were not able to investigate extremely small \hbar due to computer limitations.

Thus, using an iterative approach to long-time semiclassical calculations, we have been able to see explicitly semiclassical localization in classically diffusive systems at small \hbar . We can now say definitively that although details of long-time quantum dynamics are affected by diffraction and tunneling corrections, the essence of the localization phenomenon is indeed contained in the interference among long classical paths.

This research was supported by the National Science Foundation under Grant No. 66-701-7557-2-30. Some of the work was performed during a stay at the Weizmann Institute in Israel. The author is very grateful to E. J. Heller for many useful discussions on semiclassical methods.

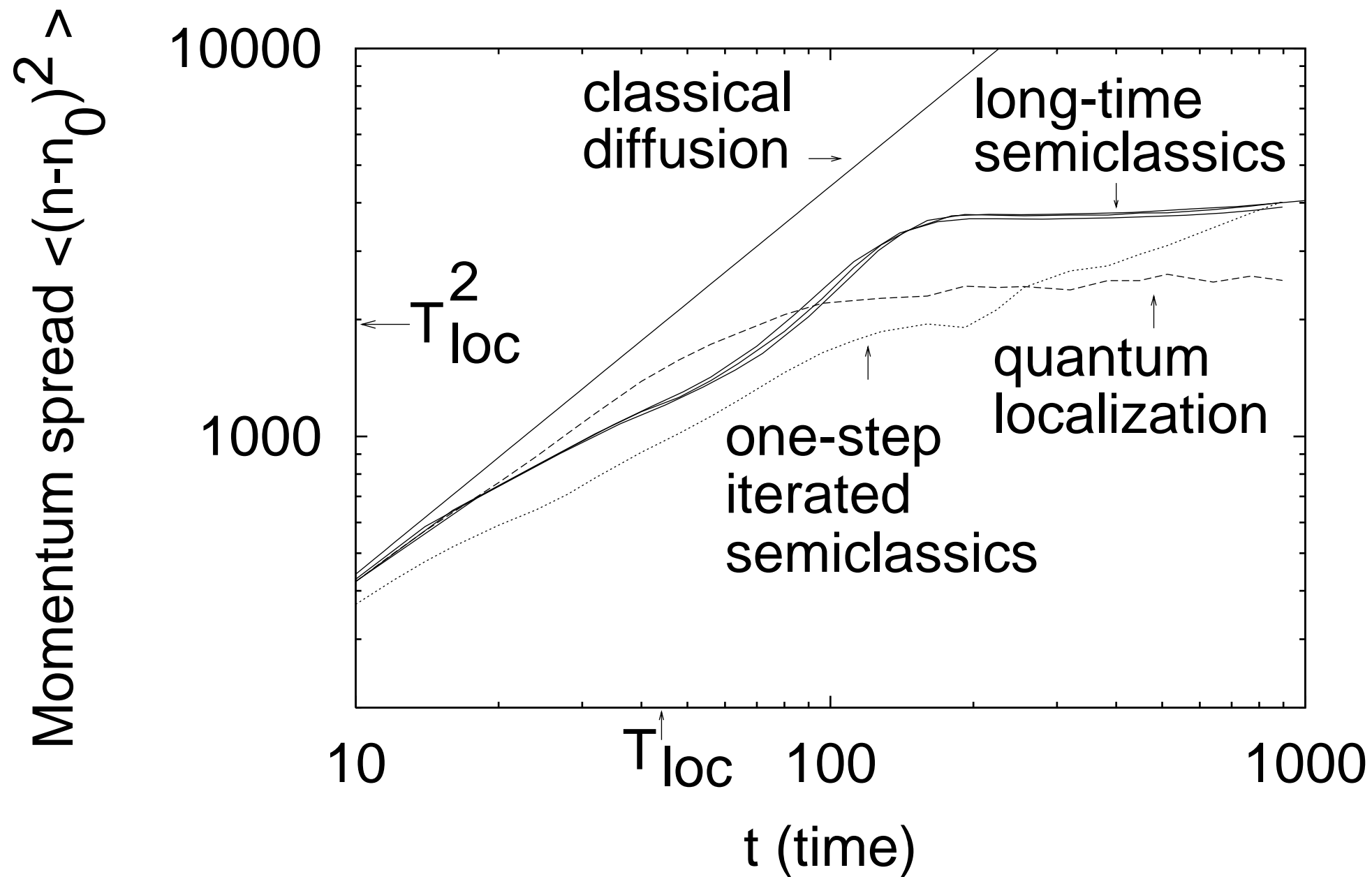
- [9] L. Kaplan, “Multiplicative semiclassical dynamics and the quantization time”, *Phys. Rev.* **E 58**, 2983 (1998).
- [10] E. B. Bogomolny, *Comm. At. Mol. Phys.* **25**, 67 (1990).
- [11] M. V. Berry, N. L. Balazs, M. Tabor, and A. Voros, *Ann. Phys. (N. Y.)* **122**, 122 (1979).

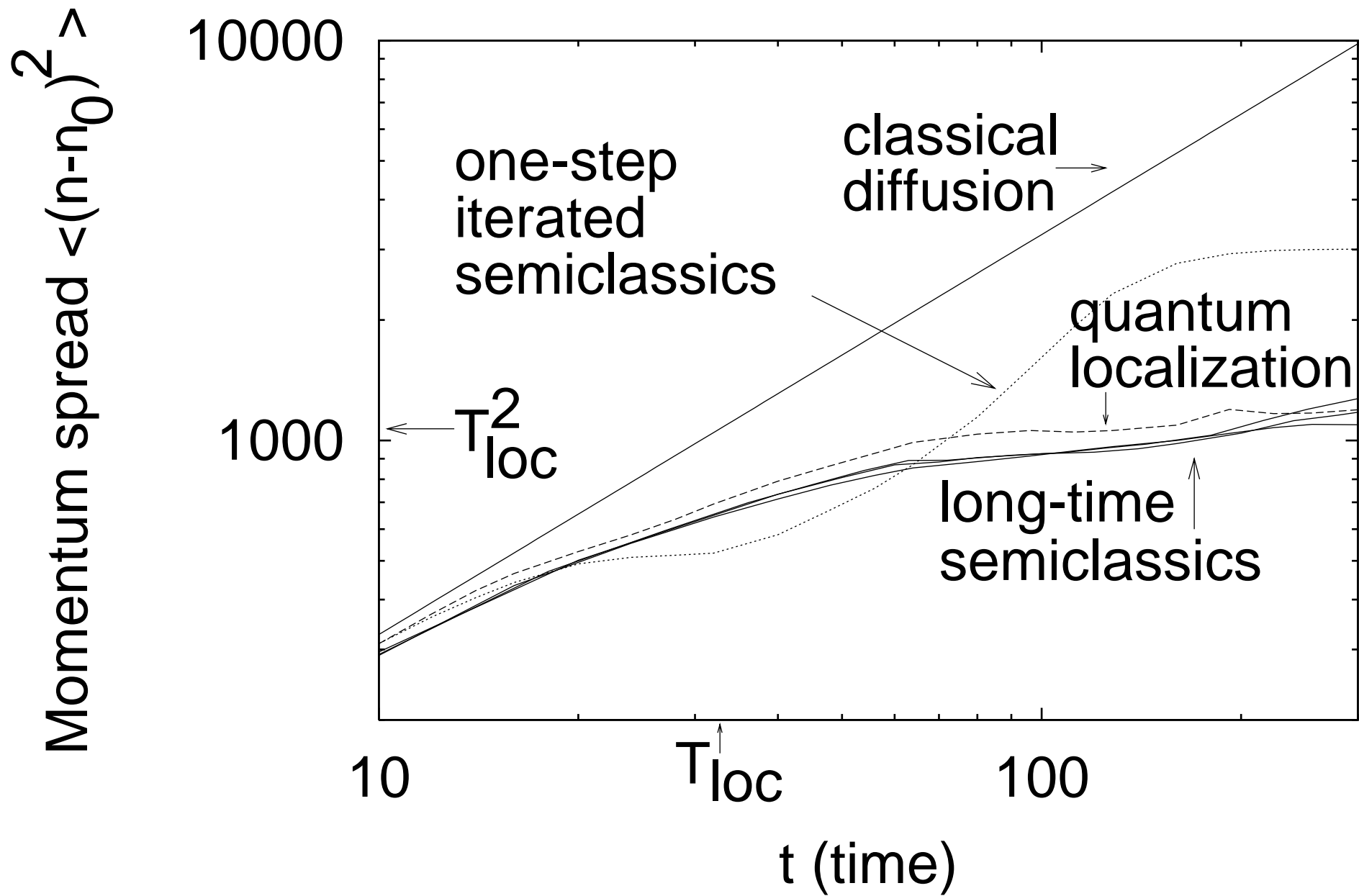
FIG. 1. Momentum spread $\langle(n - n_0)^2\rangle$ (as defined by Eq. 11), as a function of time for a kicked system with kick potential parameters $K = 1.073$, $B = 0.0$ (Eq. 6). Classical diffusion (Eq. 7) appears as a straight line; the quantum calculation, represented by a dashed curve, shows dynamical localization at time scale $T_{loc} = 44.1$. Successive approximations to the long-time semiclassical propagator (using $T_Q = 7, 8, 9$) are drawn as solid curves. The one-step iterated semiclassical propagator ($T_Q = 1$) produces the dotted curve.

FIG. 2. Same as previous Figure, with sinusoidal perturbation in the potential, $B = 0.52$. Here the expected value of T_{loc} is 32.7. Approximations to long-time semiclassical propagation using $T_Q = 8, 9, 10$ are shown as solid curves.

FIG. 3. Average RMS eigenstate width for successive approximations to long-time semiclassical propagation, $T_Q = 3 \dots 9$. The average eigenstate width for the one-step iterated propagator ($T_Q = 1$) is also displayed, as is the quantum result ($T_Q = 0$). Plusses represent the case $B = 0.0$; squares represent $B = 0.52$.

-
- [1] G. Casati, B. V. Chirikov, F. M. Izrailev, and J. Ford, in *Stochastic Behavior in Classical and Quantum Hamiltonian Systems*, ed. by G. Casati and J. Ford, Springer, New York (1979).
 - [2] B. V. Chirikov, F. M. Izrailev, and D. L. Shepelyansky, *Sov. Sci. Rev Sect. C* **2**, 209 (1982); B. V. Chirikov, *Chaos* **1**, 95 (1991); G. Casati and L. Molinari, *Prog. Theor. Phys. Suppl.* **98**, 322 (1989); M. Zaslavsky, *Chaos* **6**, 184 (1996); F. Benvenuto, G. Casati, and D. L. Shepelyansky, *Phys. Rev. A* **55**, 1732 (1997); M. El Ghafar, P. Torma, V. Savichev, E. Mayr, A. Zeiler, and W. P. Schleich, *Phys. Rev Lett.* **78**, 4181 (1997).
 - [3] F. L. Moore, J. C. Robinson, C. F. Bharucha, B. Sundaram, and M. G. Raizen, *Phys. Rev. Lett.* **74**, 4598 (1995); F. L. Moore, J. C. Robinson, C. Bharucha, P. E. Williams, and M. G. Raizen, *Phys. Rev. Lett.* **73**, 2974 (1995).
 - [4] A. Altland and M. R. Zirnbauer, *Phys. Rev. Lett.* **77**, 4536 (1996); I. Dana, E. Eisenberg, and N. Schnerb, *Phys. Rev. Lett.* **74**, 686 (1995); D. L. Shepelyansky, *Physica* **28D**, 103 (1987).
 - [5] A. Shudo and K. Ikeda, *Prog. Theor. Phys. Suppl.* **116**, 283 (1994).
 - [6] R. Scharf and B. Sundaram, *Phys. Rev. Lett.* **76**, 4907 (1996).
 - [7] D. Cohen, *J. Phys.* **A 31**, 277 (1998); D. Cohen, *Phys. Rev.* **E 55**, 1422 (1997).
 - [8] R. Scharf and B. Sundaram, *Phys. Rev. Lett.* **77**, 263 (1996).





Average RMS eigenstate width

